Di-tert-butyl tin(IV) 2-pyridyl and 4,6-dimethyl-2-pyrimidyl thiolates: versatile single source precursors for the preparation of SnS nanoplatelets as anode material for lithium ion batteries

AdishTyagi,[a,b] Gourab Karmakar,[a,b] B. P. Mandal,[a,b] Dipa Dutta Pathak,[a,b]Amey Wadawale,[a] G. Kedarnath,[a,b] A. P. Srivastava[c] and Vimal K. Jain[a,d]

[a]*Chemistry Division, Bhabha Atomic Research Centre, Mumbai- 400 085 (India),*
[b]*HomiBhabha National Institute, Anushaktinagar, Mumbai- 400 094 (India)*
[c]*Materials Science Division, Bhabha Atomic Research Centre, Mumbai- 400 085 (India).*
[d]*UM-DAE Centre for Excellence in Basic Sciences, University of Mumbai, Kalina Campus, Mumbai-400 098 (India)*

Figure Captions

*Figure S1 ^{1}H NMR spectrum of $[^{t}Bu_2Sn(Spy)_2]$ (**1**) acquired in $CDCl_3$.*

*Figure S2 $^{13}C\{^{1}H\}$ NMR spectrum of $[^{t}Bu_2Sn(Spy)_2]$ (**1**) acquired in $CDCl_3$.*

*Figure S3 $^{119}Sn\{^{1}H\}$ NMR spectrum of $[^{t}Bu_2Sn(Spy)_2]$ (**1**) acquired in $CDCl_3$.*

*Figure S4 ^{1}H NMR spectrum of $[^{t}Bu_2SnCl(Spy)]$ (**2**) acquired in $CDCl_3$.*

*Figure S5 $^{13}C\{^{1}H\}$ NMR spectrum of $[^{t}Bu_2SnCl(Spy)]$ (**2**) acquired in $CDCl_3$.*

*Figure S6 $^{119}Sn\{^{1}H\}$ NMR spectrum of $[^{t}Bu_2SnCl(Spy)]$ (**2**) acquired in $CDCl_3$.*

*Figure S7 ^{1}H NMR spectrum of $[^{t}Bu_2SnCl(SpymMe_2)]$ (**3**) acquired in $CDCl_3$.*

*Figure S8 $^{13}C\{^{1}H\}$ NMR spectrum of $[^{t}Bu_2SnCl(SpymMe_2)]$ (**3**) acquired in $CDCl_3$.*

*Figure S9 $^{119}Sn\{^{1}H\}$ NMR spectrum of $[^{t}Bu_2SnCl(SpymMe_2)]$ (**3**) acquired in $CDCl_3$.*

*Figure S 10 Disorder molecular structure of $[^{t}Bu_2Sn(Spy)_2]$ (**1**) mirrored through (202) plane.*

*Figure S11 EDS spectrum of SnS nanoplatelets prepared from the thermolysis of $[^{t}Bu_2Sn(Spy)_2]$ (**1**) in OAm.*

*Figure S12 EDS spectrum of SnS nanoplatelets prepared from the thermolysis of $[^{t}Bu_2SnCl(Spy)]$ (**2**) in OAm.*

*Figure S13 EDS spectrum of SnS nanoplatelets prepared from the thermolysis of $[^{t}Bu_2SnCl(SpymMe_2)]$ (**3**) in OAm.*

*Figure S14 XPS spectrum of SnS nanoplatelets prepared from the thermolysis of $[^{t}Bu_2SnCl(SpymMe_2)]$ (**3**) in OAm (a) survey scan, (b) Sn 3d region, (c) S 2p region.*

*Figure S15 The elemental imaging of SnS nanoplatelets obtained by the thermolysis of (a) $[^{t}Bu_2Sn(Spy)_2]$ (**1**), (b) $[^{t}Bu_2Sn(Cl)(Spy)]$ (**2**) and (c) $[^{t}Bu_2Sn(Cl)(SpymMe_2)]$ (**3**), respectively in OAm.*

*Figure S16 The SAED patterns of SnS nanoplatelets obtained by the thermolysis of (a) $[^{t}Bu_2Sn(Spy)_2]$ (**1**), (b) $[^{t}Bu_2Sn(Cl)(Spy)]$ (**2**) and (c) $[^{t}Bu_2Sn(Cl)(SpymMe_2)]$ (**3**), respectively in OAm.*

*Figure S17 pXRD spectra of orthorhombic phase of SnS thin films deposited on (a) glass and (b) silicon substrate by the AACVD of [^{t}Bu$_2$Sn(Spy)$_2$] (**1**) at 400℃ for 1 h. (c) represents the standard SnS XRD patter (JCPDS file no. 39-0354).*

Figure S18 AFM images of micro regions, 30.0 × 30.0, 10.0 × 10.0 and 5.0 × 5.0 μm^2 SnS thin film *deposited on (a,b,c) silicon and (d,e,f) glass substrate by the AACVD of [^{t}Bu$_2$Sn(Spy)$_2$] (**1**) at 400℃ for 1 h.*

*Figure S19 Estimation of lithium diffusion coefficient of SnS nanoplatelets obtained from the thermolysis of [^{t}Bu$_2$Sn(Spy)$_2$] (**1**). Linear relation between Z' and square root of frequency. The warburg constant (σ) could be obtained from the slop of the plot.*

Figure S20 Electrochemical performance of SnS anode after removal of capping agent.

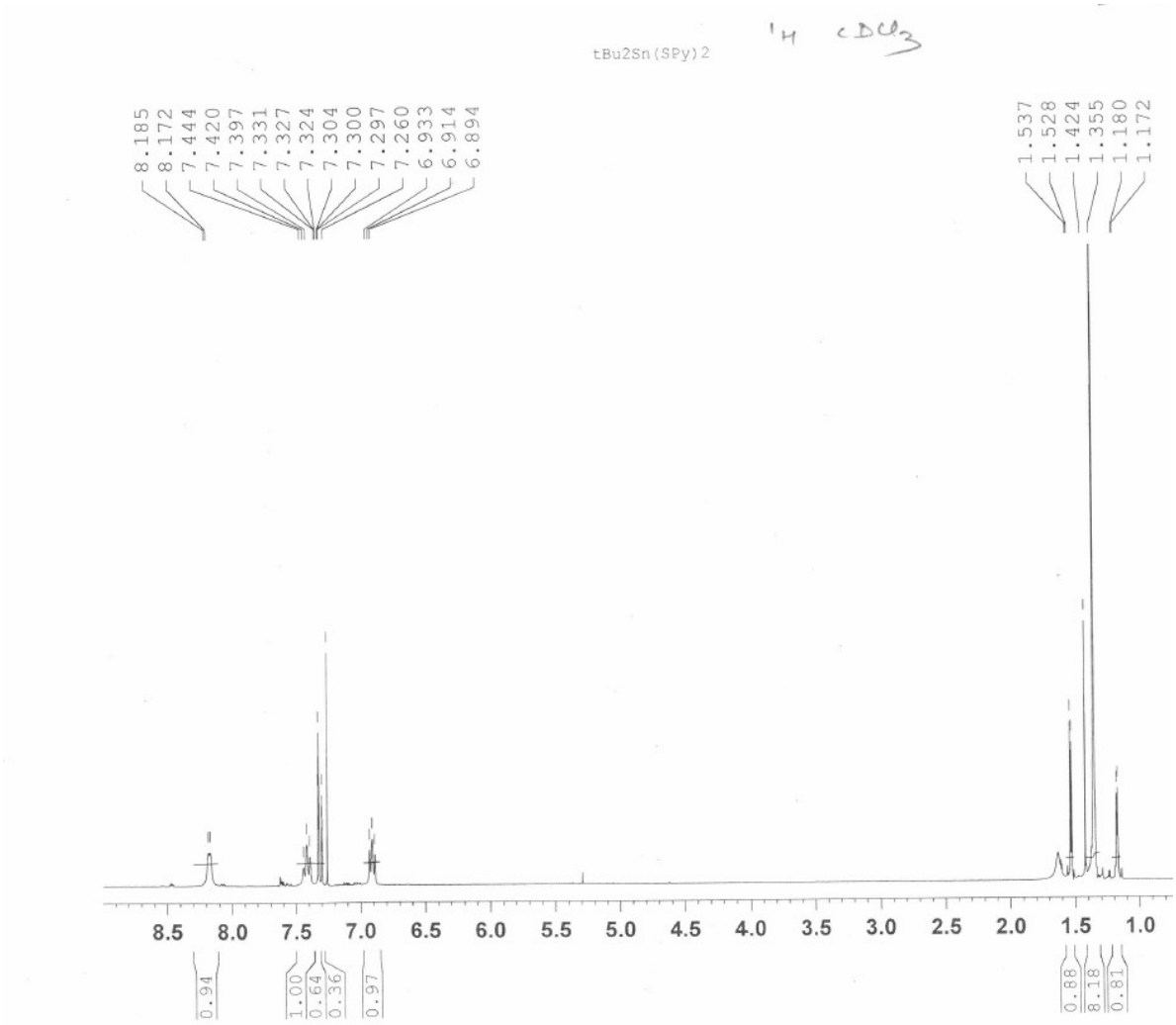

*Figure S1 ^{1}H NMR spectrum of [^{t}Bu$_2$Sn(Spy)$_2$] (**1**) acquired in CDCl$_3$.*

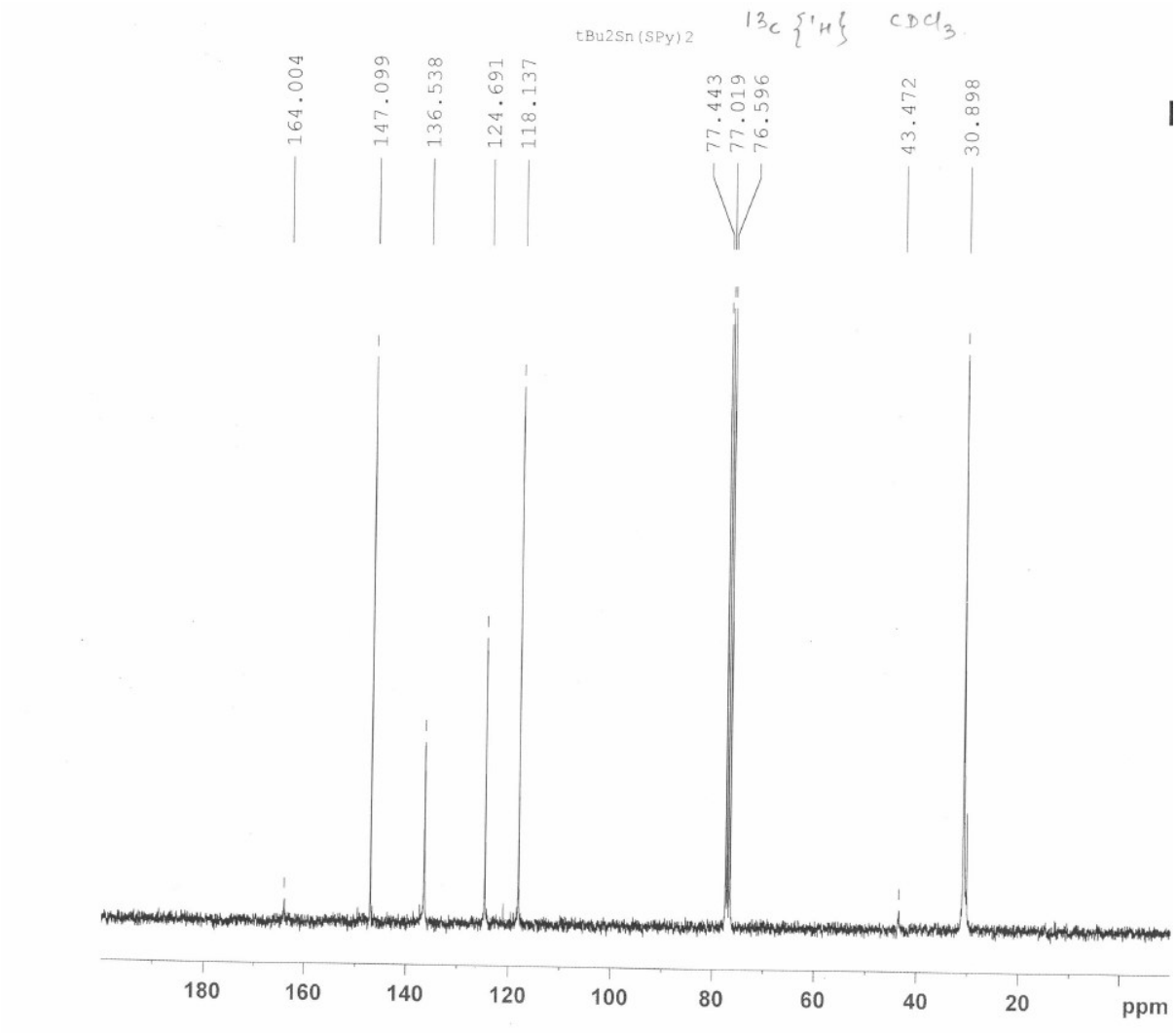

*Figure S2 $^{13}C\{^{1}H\}$ NMR spectrum of [$^{t}Bu_2Sn(Spy)_2$] (**1**) acquired in $CDCl_3$.*

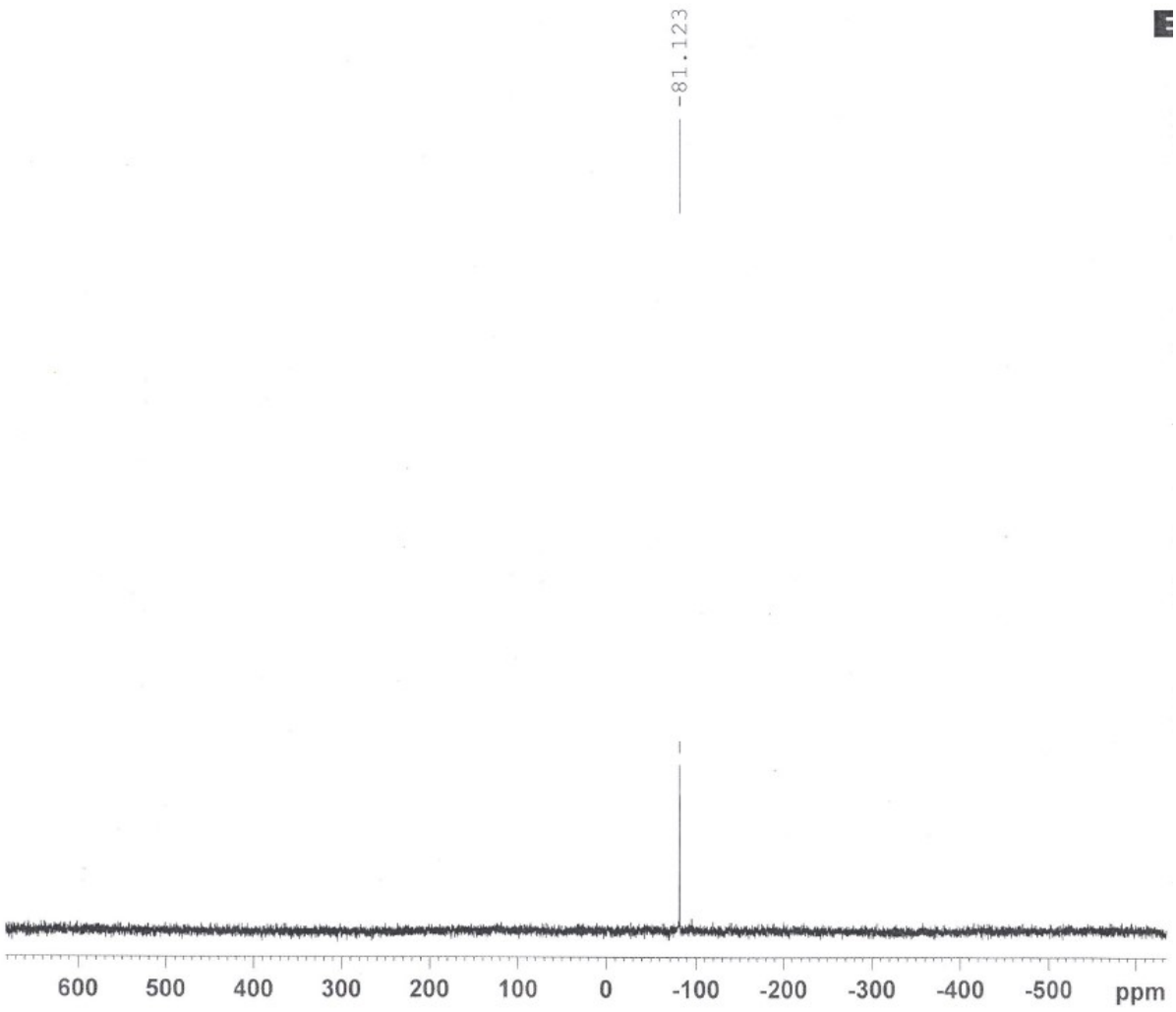

*Figure S3 $^{119}Sn\{^{1}H\}$ NMR spectrum of [$^{t}Bu_2Sn(Spy)_2$] (**1**) acquired in $CDCl_3$.*

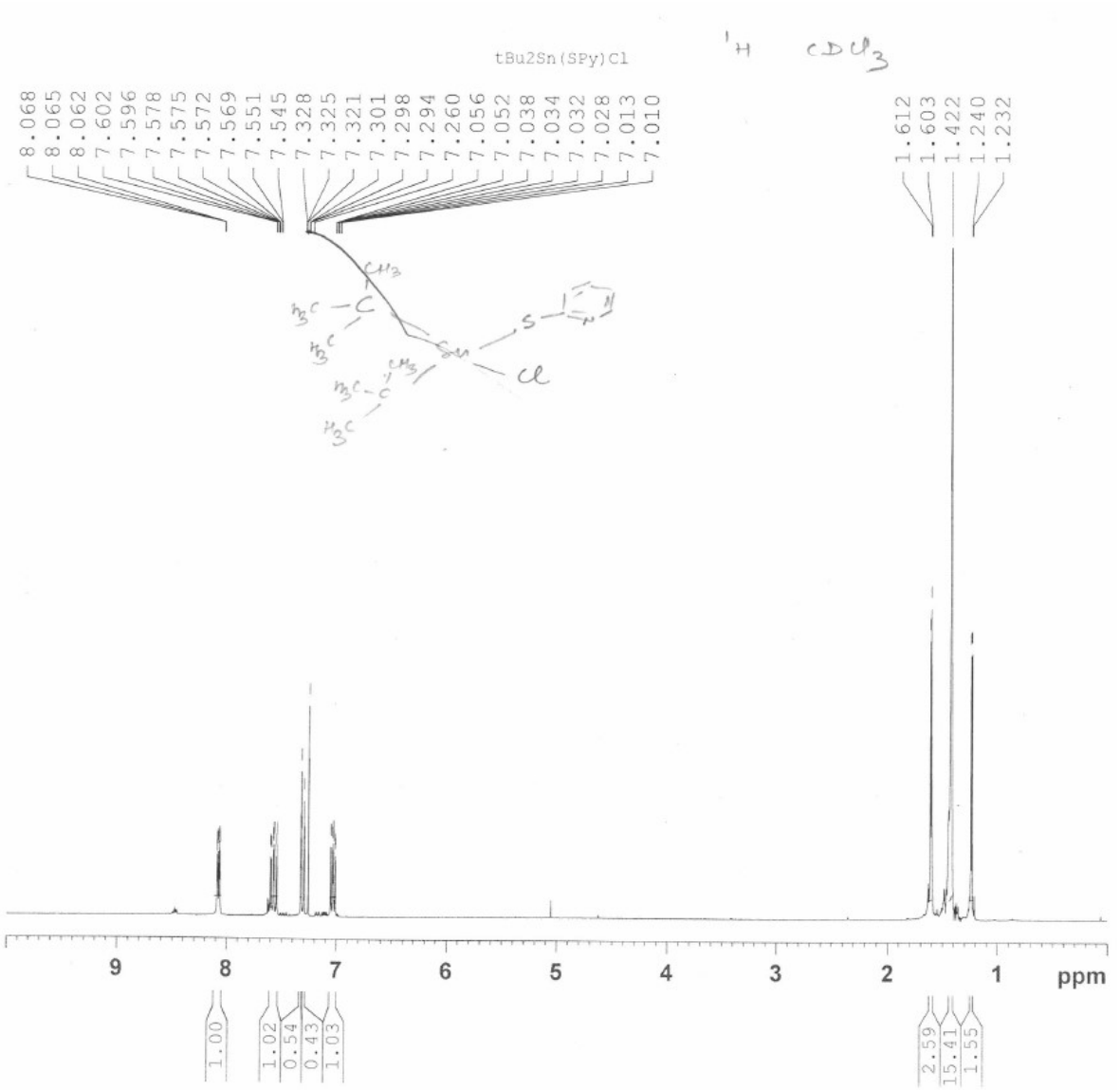

*Figure S4 ^{1}H NMR spectrum of [$^{t}Bu_2SnCl(Spy)$] (**2**) acquired in $CDCl_3$.*

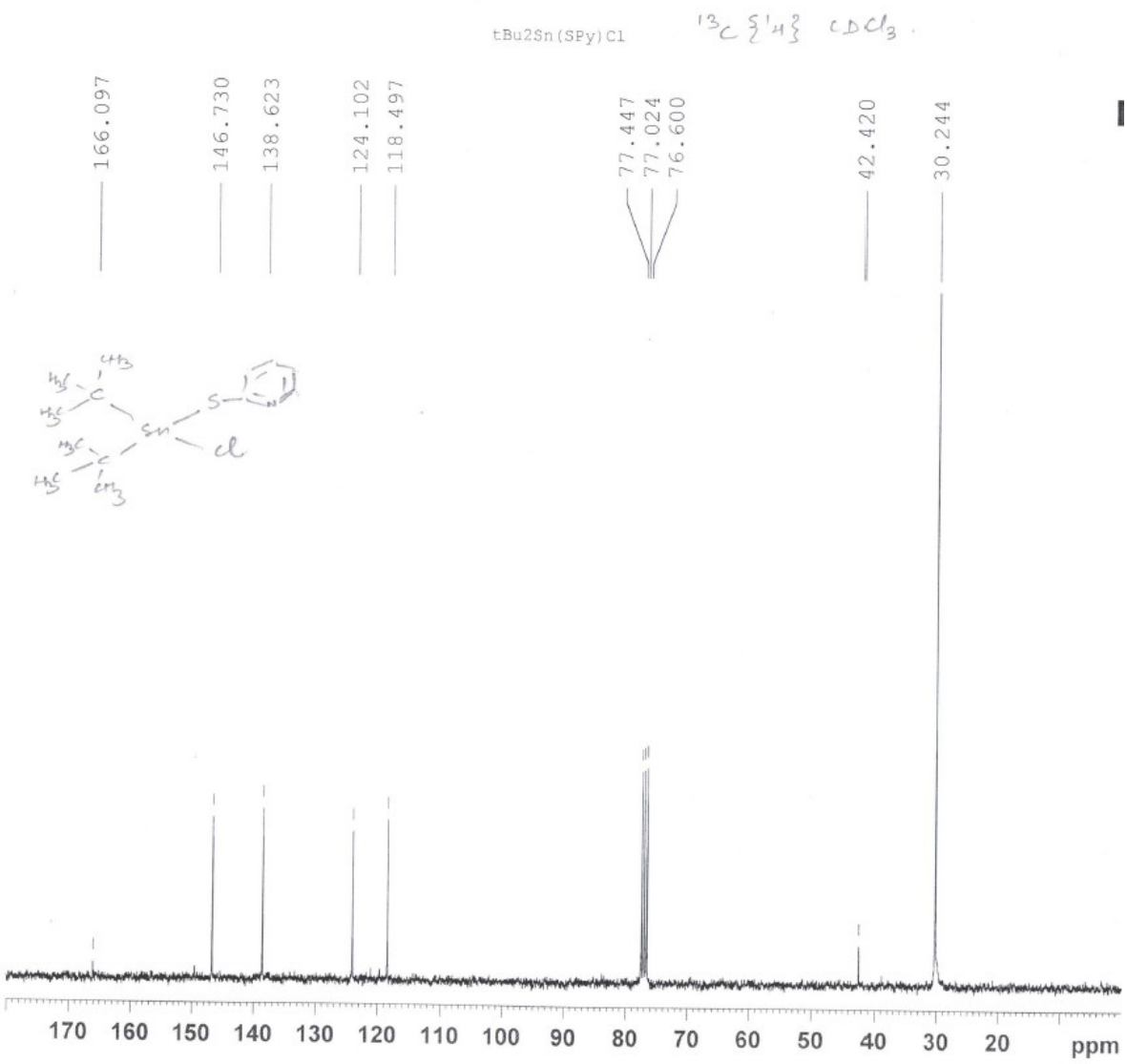

*Figure S5 $^{13}C\{^{1}H\}$ NMR spectrum of [$^{t}Bu_2SnCl(Spy)$] (**2**) acquired in $CDCl_3$.*

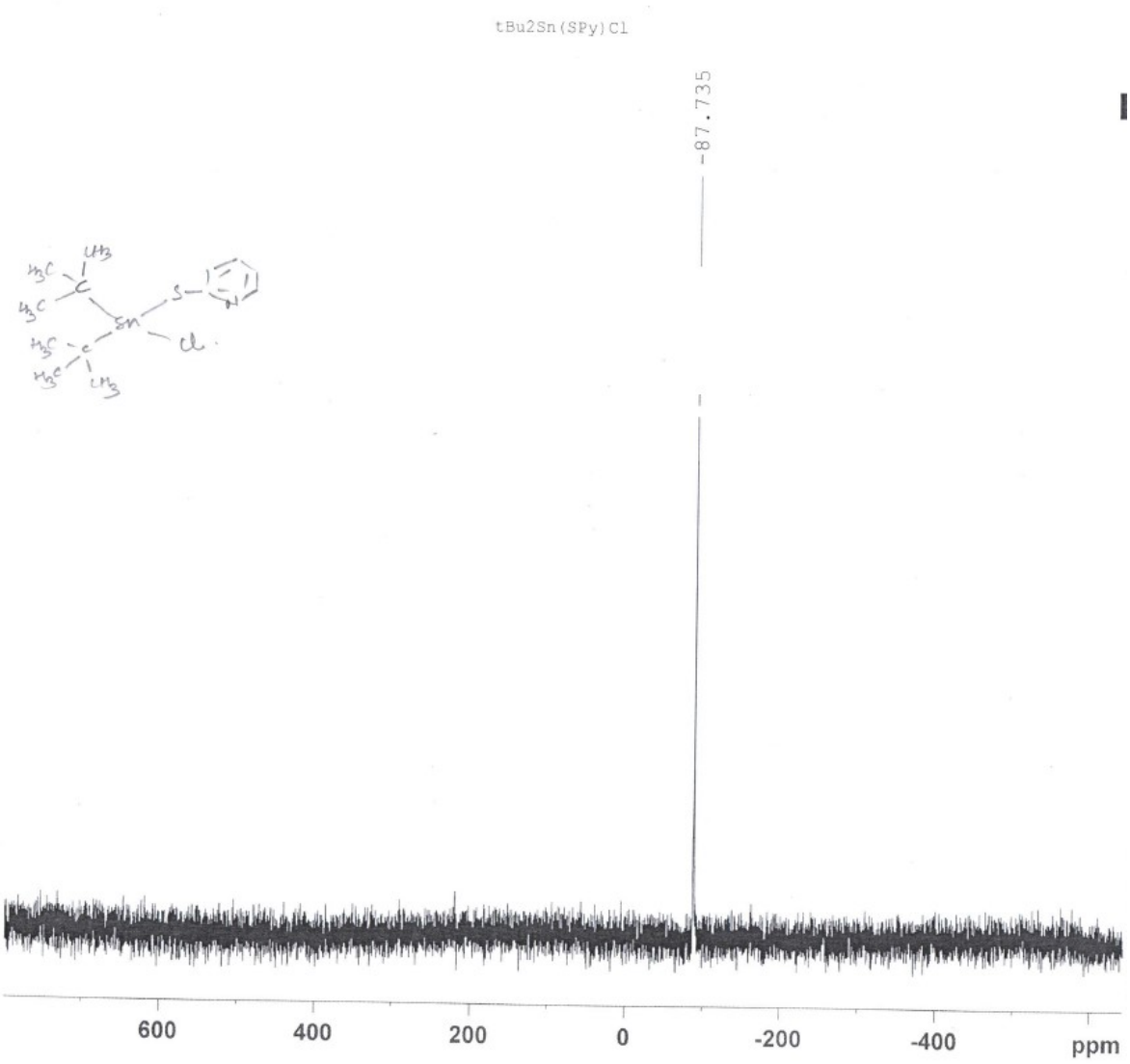

*Figure S6 $^{119}Sn\{^{1}H\}$ NMR spectrum of [$^{t}Bu_2SnCl(Spy)$] (**2**) acquired in $CDCl_3$.*

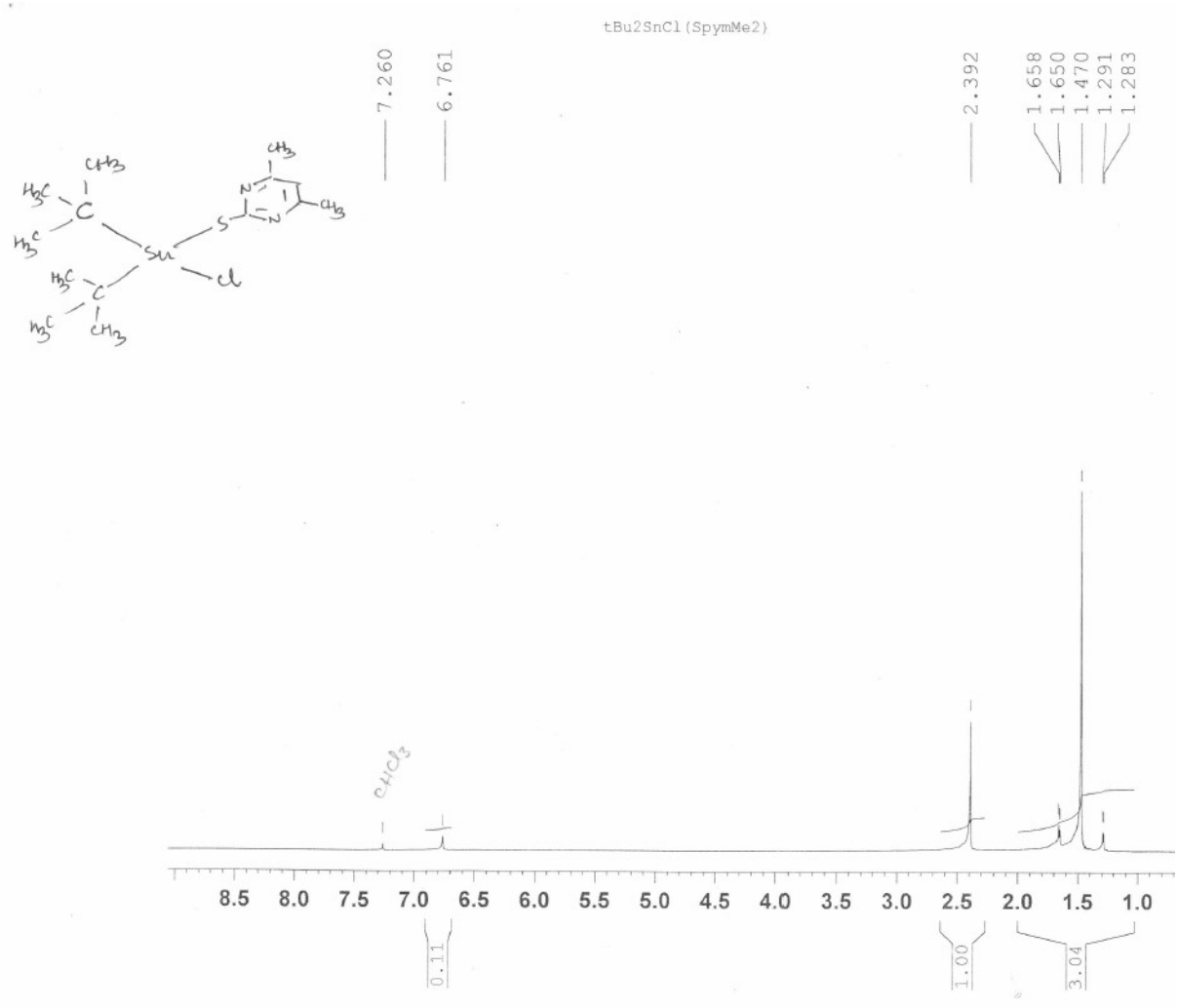

*Figure S7 ^{1}H NMR spectrum of [$^{t}Bu_2SnCl(SpymMe_2)$] (**3**) acquired in $CDCl_3$.*

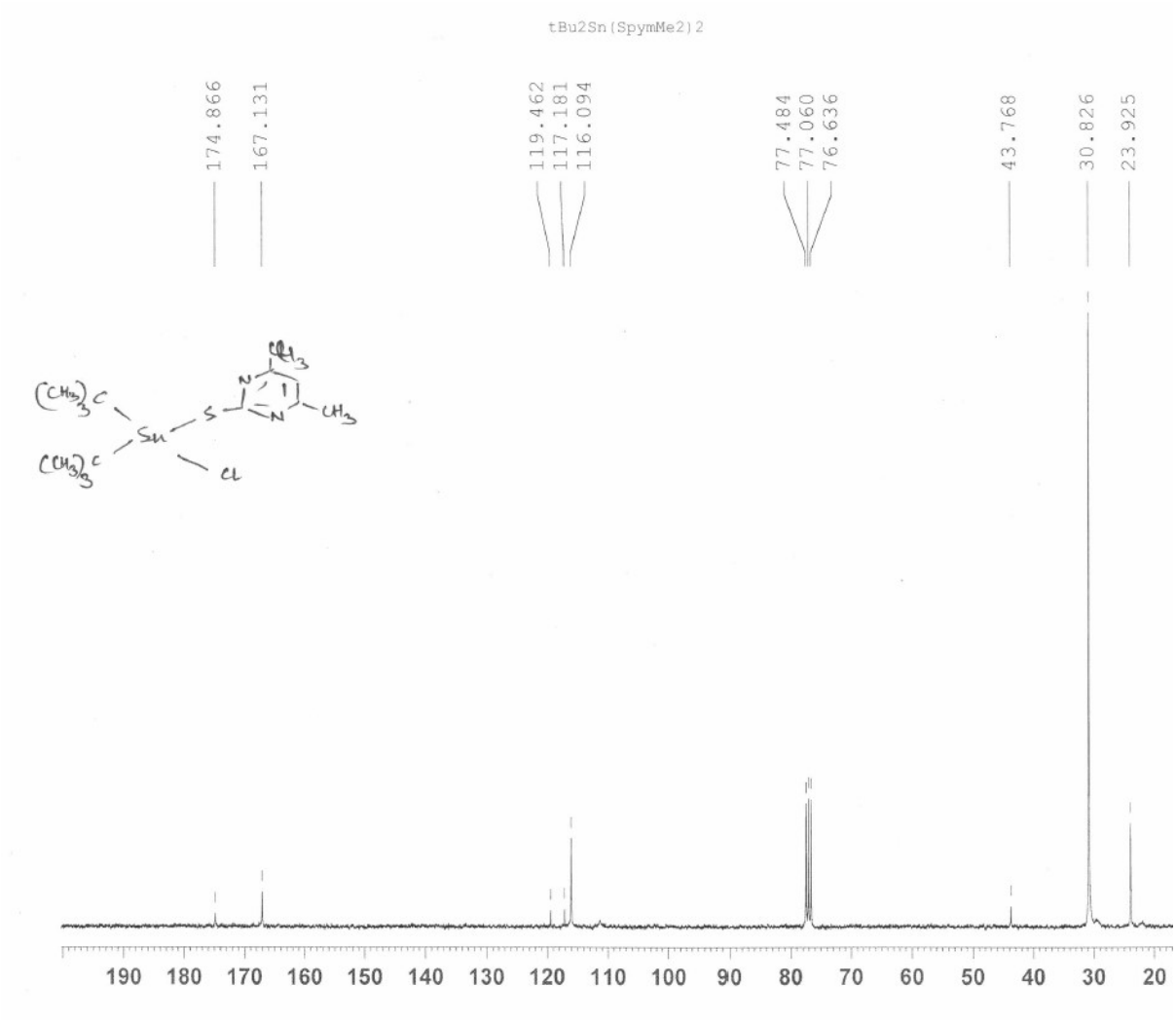

*Figure S8 $^{13}C\{^{1}H\}$ NMR spectrum of [$^{t}Bu_2SnCl(SpymMe_2)$] (**3**) acquired in $CDCl_3$.*

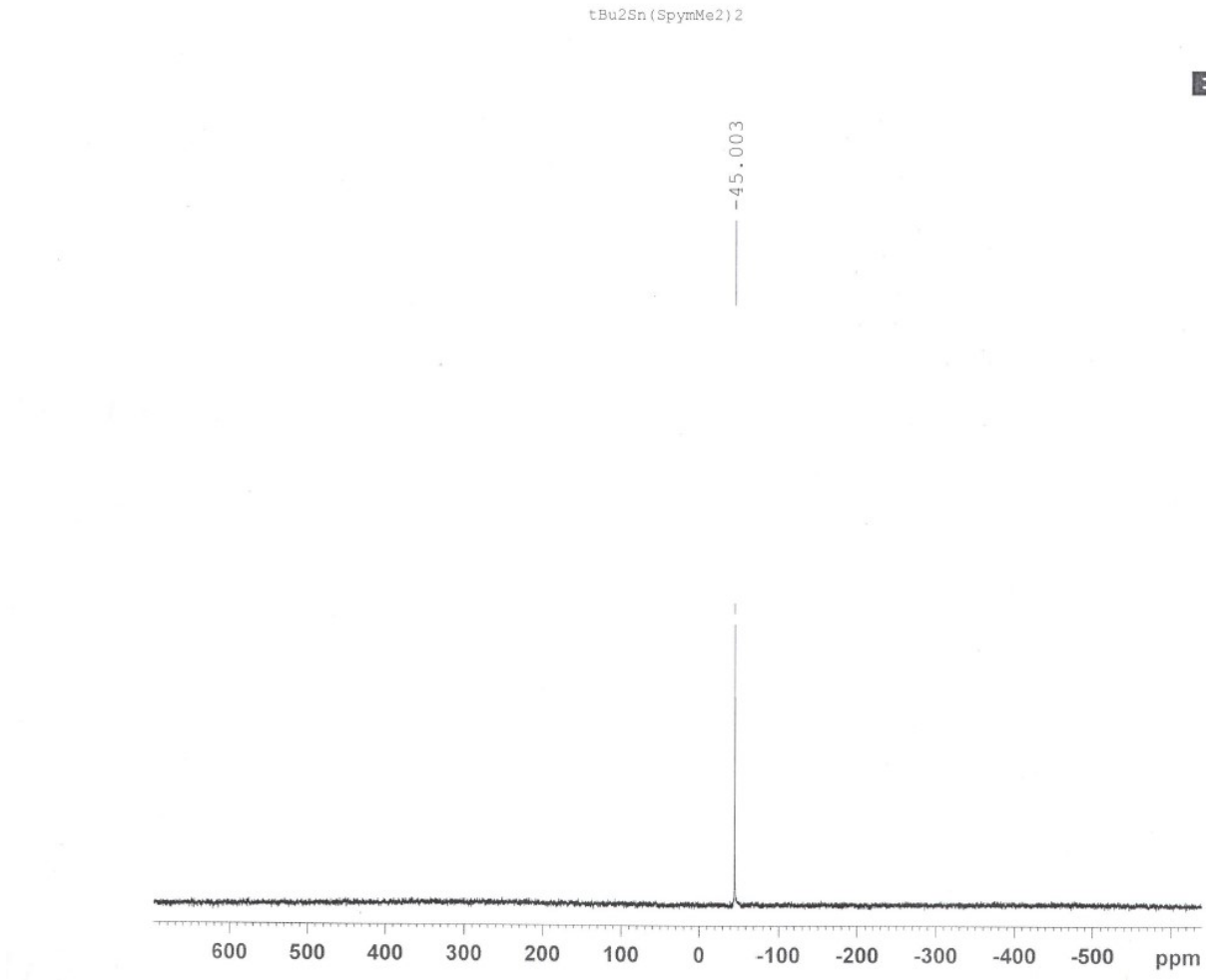

*Figure S9 $^{119}Sn\{^{1}H\}$ NMR spectrum of [$^{t}Bu_2SnCl(SpymMe_2)$] (**3**) acquired in $CDCl_3$.*

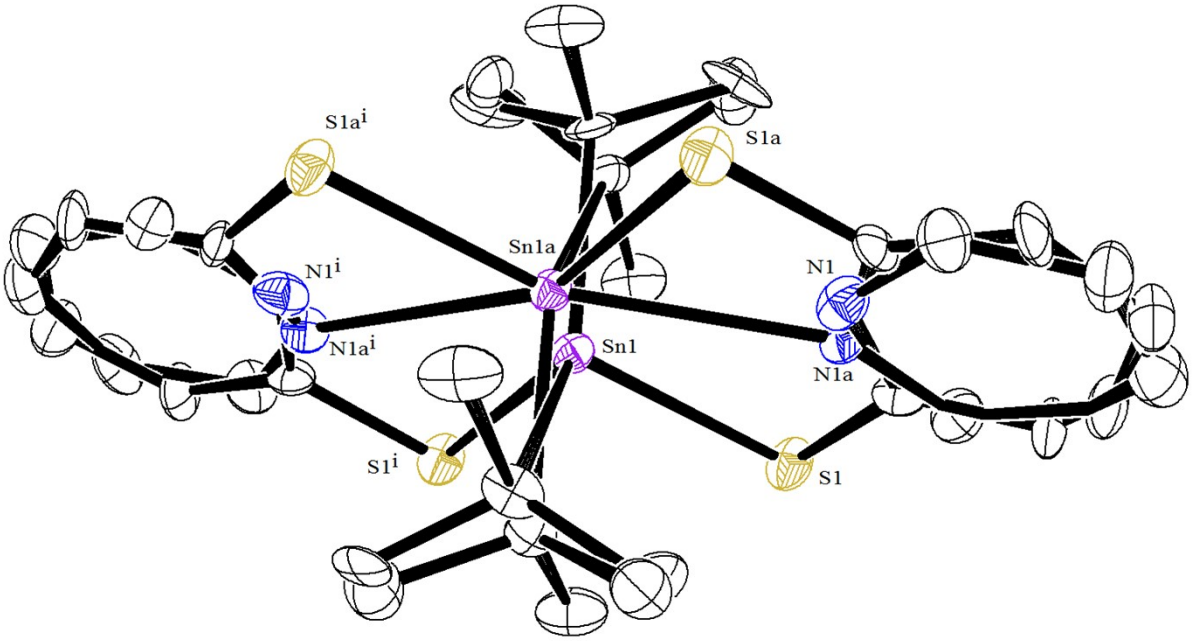

Figure S 10 Disorder molecular structure of [$^{t}Bu_2Sn(Spy)_2$] (1) mirrored through (202) plane.

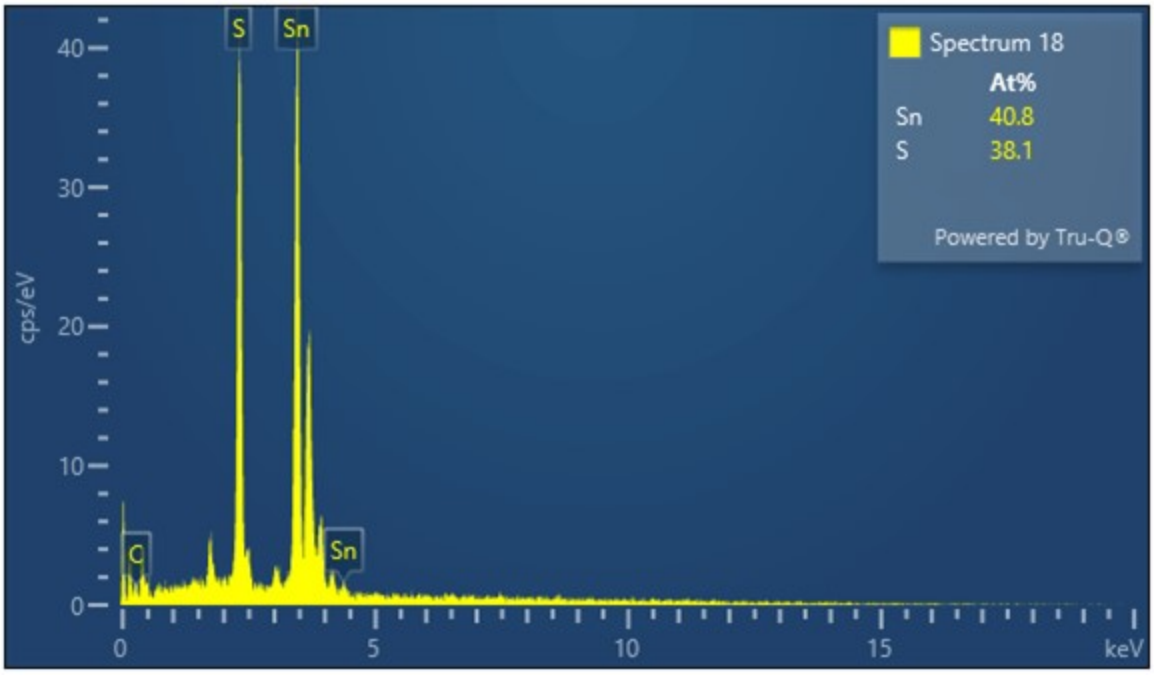

*Figure S11 EDS spectrum of SnS nanoplatelets prepared from the thermolysis of [^{t}Bu$_2$Sn(Spy)$_2$] (**1**) in OAm.*

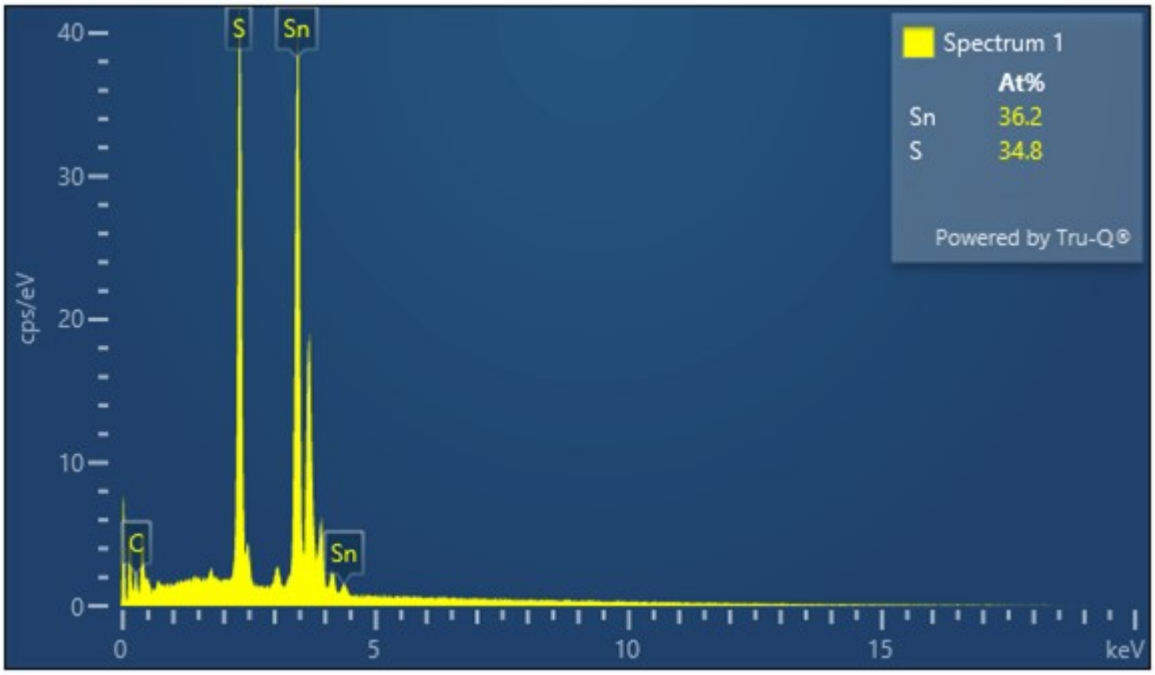

*Figure S12 EDS spectrum of SnS nanoplatelets prepared from the thermolysis of [^{t}Bu$_2$SnCl(Spy)] (**2**) in OAm.*

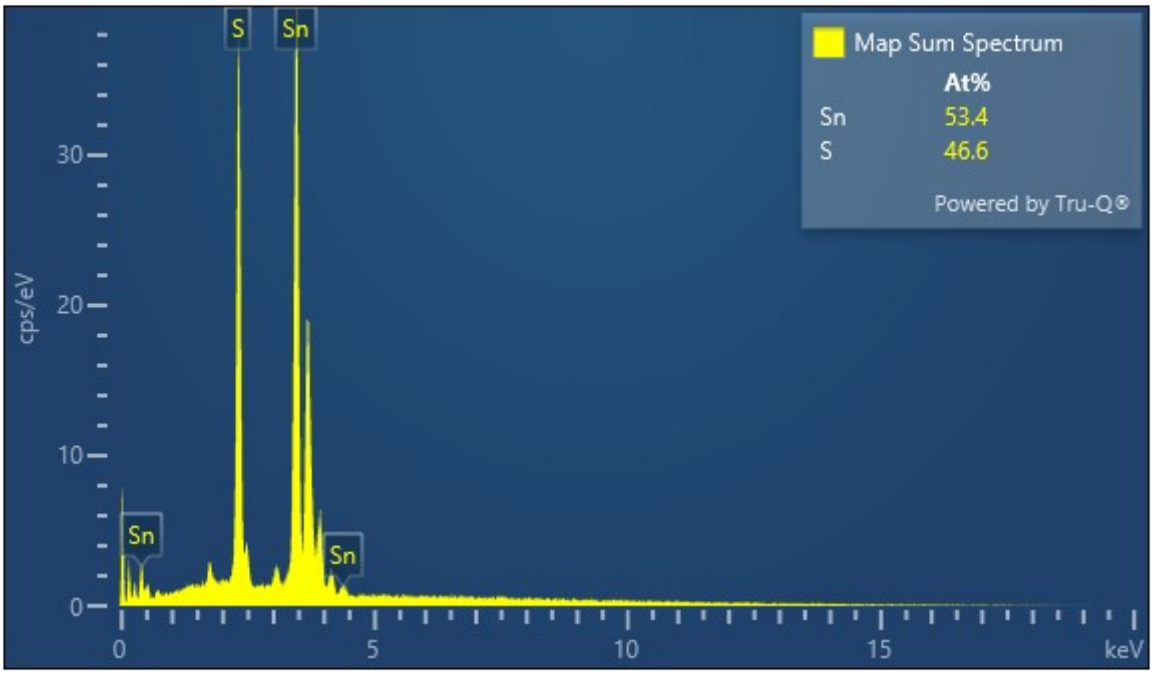

*Figure S13 EDS spectrum of SnS nanoplatelets prepared from the thermolysis of [$^{t}Bu_2SnCl(SpymMe_2)$] (**3**) in OAm.*

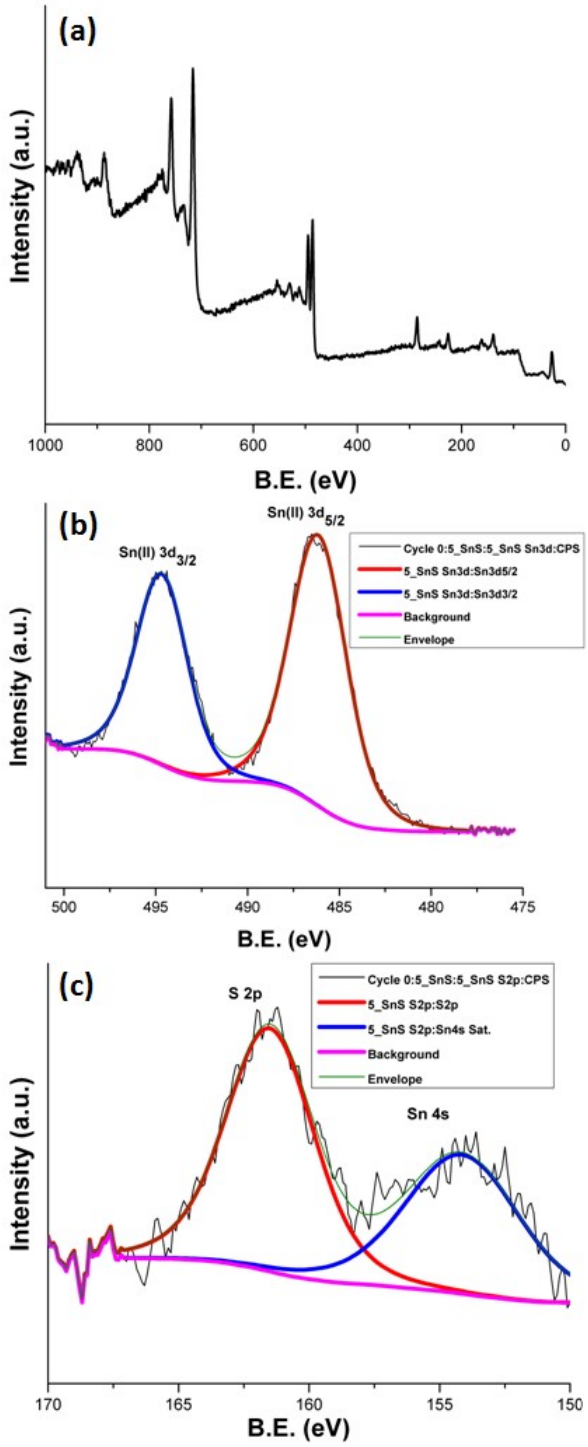

*Figure S14 XPS spectrum of SnS nanoplatelets prepared from the thermolysis of [^{t}Bu$_2$SnCl(SpymMe$_2$)] (**3**) in OAm (a) survey scan, (b) Sn 3d region, (c) S 2p region.*

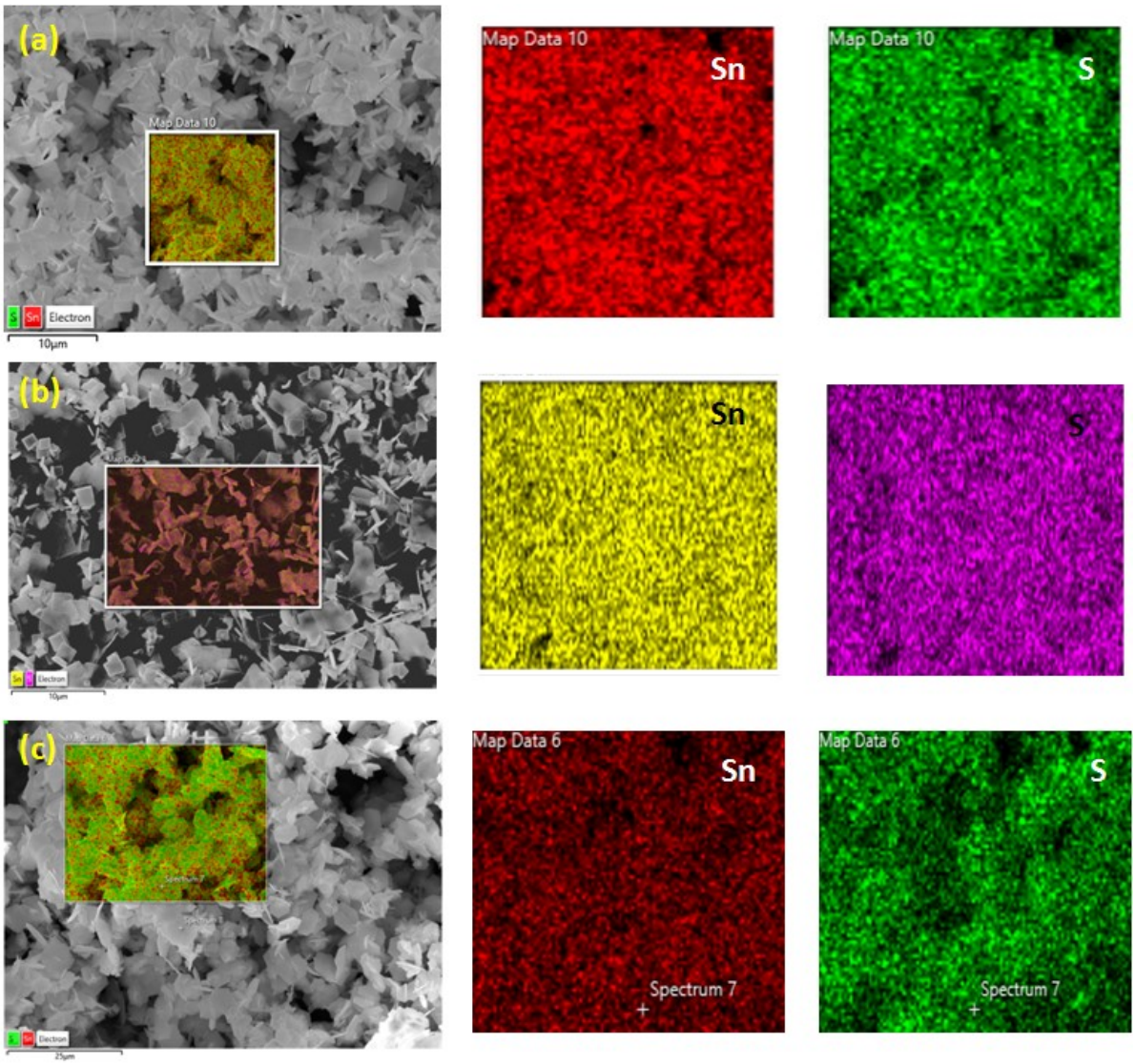

*Figure S15 The elemental imaging of SnS nanoplatelets obtained by the thermolysis of (a) [^{t}Bu$_2$Sn(Spy)$_2$] (**1**), (b) [^{t}Bu$_2$Sn(Cl)(Spy)] (**2**) and (c) [^{t}Bu$_2$Sn(Cl)(SpymMe$_2$)] (**3**), respectively in OAm.*

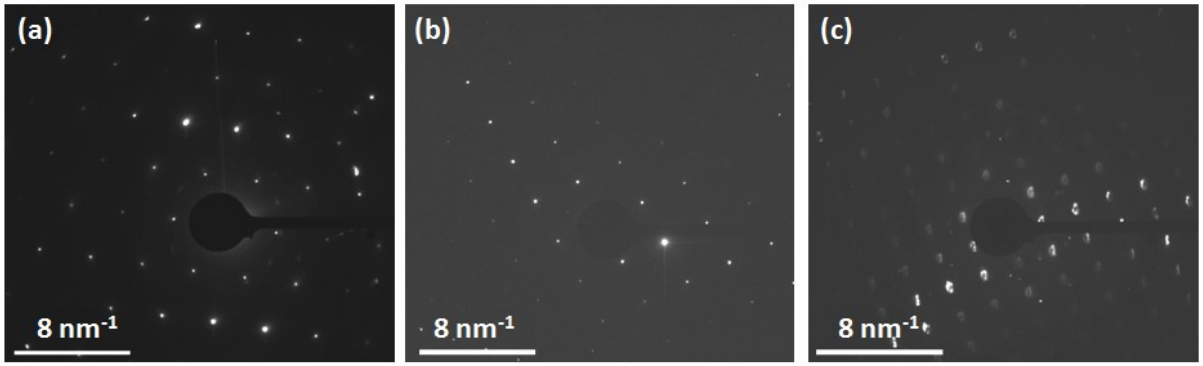

*Figure S16 The SAED patterns of SnS nanoplatelets obtained by the thermolysis of (a) [^{t}Bu$_2$Sn(Spy)$_2$] (**1**), (b) [^{t}Bu$_2$Sn(Cl)(Spy)] (**2**) and (c) [^{t}Bu$_2$Sn(Cl)(SpymMe$_2$)] (**3**), respectively in OAm.*

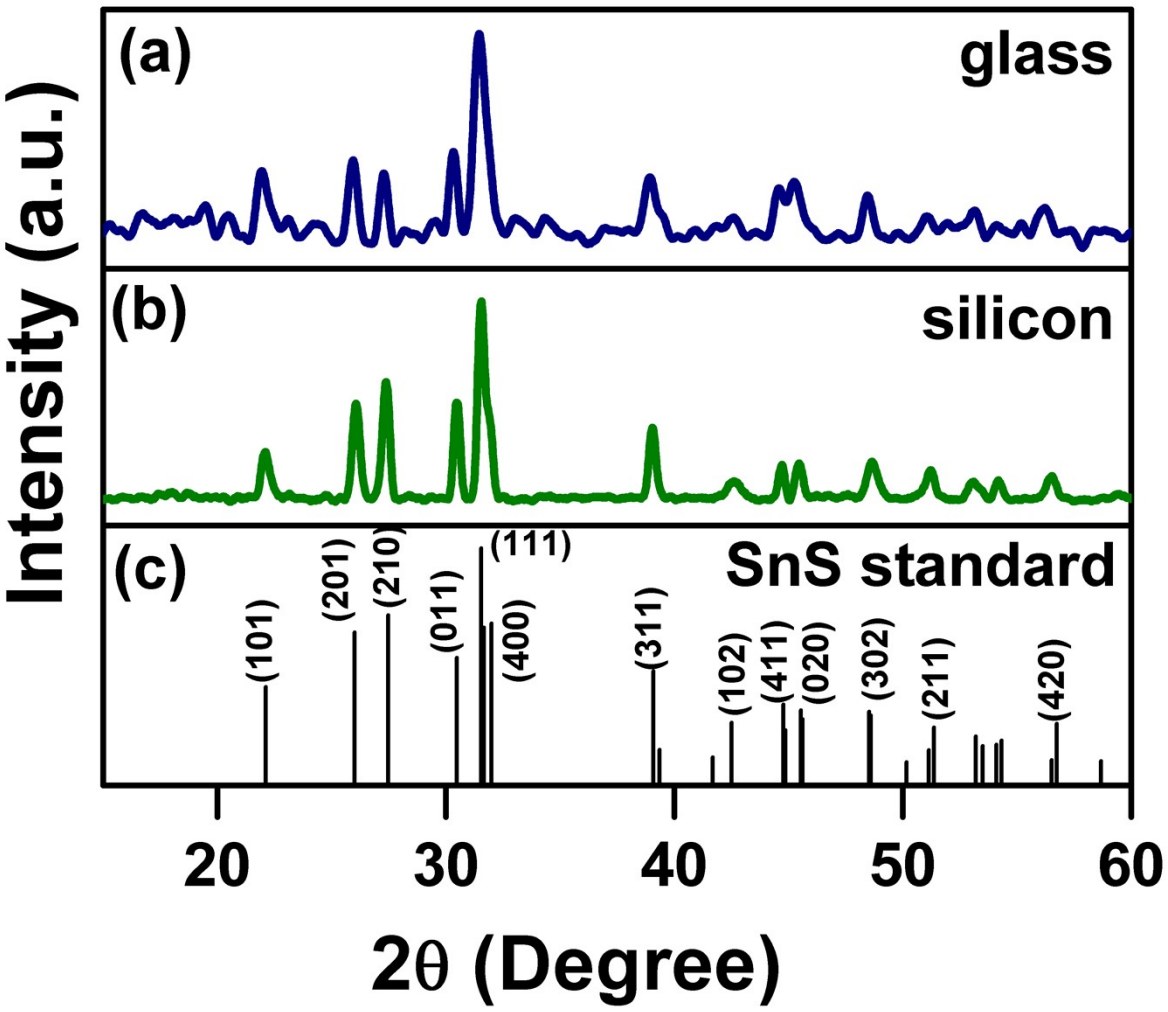

*Figure S17 pXRD spectra of orthorhombic phase of SnS thin films deposited on (a) glass and (b) silicon substrate by the AACVD of [^{t}Bu$_2$Sn(Spy)$_2$] (**1**) at 400 ℃ for 1 h. (c) represents the standard SnS XRD patter (JCPDS file no. 39-0354).*

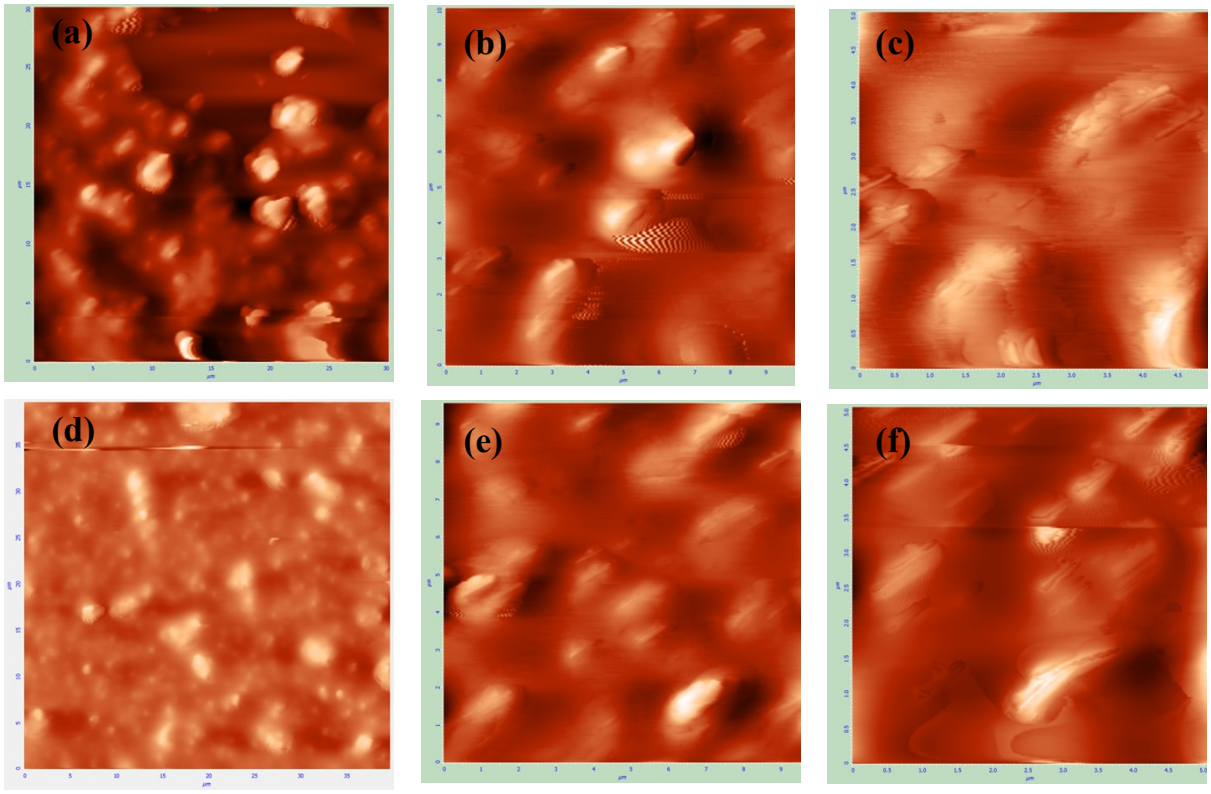

*Figure S18 AFM images of micro regions, 30.0 × 30.0, 10.0 × 10.0 and 5.0 × 5.0 μm² SnS thin film deposited on (a,b,c) silicon and (d,e,f) glass substrate by the AACVD of [$^{t}Bu_2Sn(Spy)_2$] (**1**) at 400 ℃ for 1 h.*

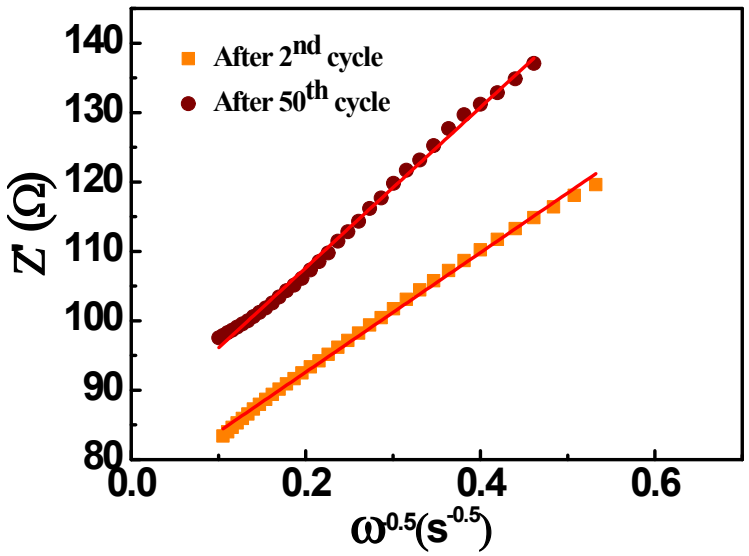

*Figure S19 Estimation of lithium diffusion coefficient of SnS nanoplatelets obtained from the thermolysis of [$^{t}Bu_2Sn(Spy)_2$] (**1**). Linear relation between Z' and square root of frequency. The warburg constant (σ) could be obtained from the slop of the plot.*

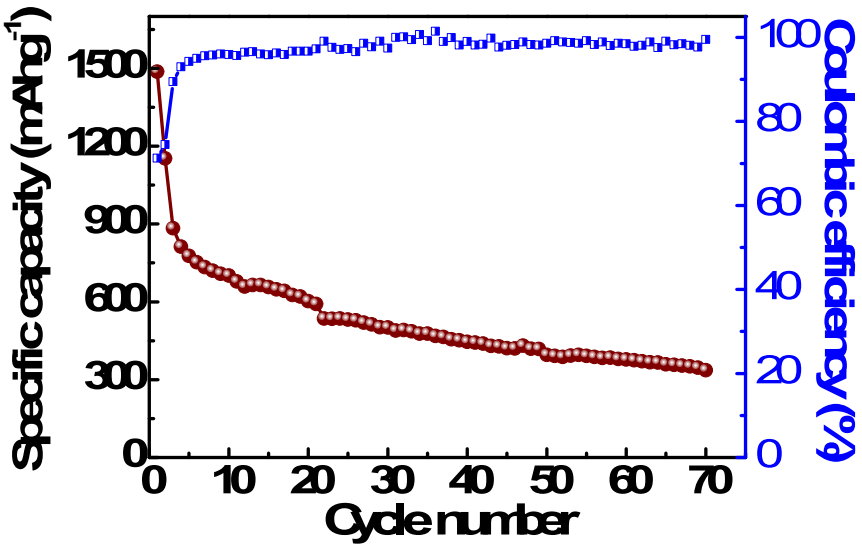

Figure S20 Electrochemical performance of SnS anode after removal of capping agent.

Table T1: Roughness of SnS *thinfilm* obtained from AFM data.

Substrate	Micro-area scanned (μm^2)	Average roughness (nm)
Silicon	30.0 × 30.0 10.0 × 10.0 5.0 ×5.0	175 86.9 31.3
Glass	30.0 × 30.0 10.0 × 10.0 5.0 ×5.0	178.9 133.7 47.4